Multi-Objective Topology Optimization of Composite Structures Considering Resin Filling Time

Yuqing Zhou[1], **Kazuhiro Saitou**[2]

[1] University of Michigan, Ann Arbor, USA, yuqingz@umich.edu
[2] University of Michigan, Ann Arbor, USA, kazu@umich.edu

1. Abstract
This paper presents multi-objective topology optimization of composite structures manufactured by resin transfer molding. The problem is formulated as minimizing both structural compliance and resin filling time. The empirical model of resin filling process is constructed by mining the results of numerical process simulations of massively sampled structural topologies within a fixed bounding box, using Random Forest statistical learning. Thanks to the abstract topology features inspired by underlying physics of the filling process, the resulting process model is far more generalizable than the traditional surrogate models based on, *e.g.*, bitmap and local feature representation, with no penalty in computation time. In particular, the model can reasonably be applied to the situations with the different inlet gate locations and initial bounding boxes from the training samples, while the traditional surrogate models completely fail in such situations.
Three case studies for composite structure topology optimization are discussed with different inlet gate locations and initial bounding boxes in order to demonstrate the robustness of the developed process model. The multi-objective topology optimization problem is solved by the Kriging-interpolated level-set approach and multi-objective genetic algorithm (MOGA). The resulting Pareto frontiers offer opportunities to select the designs with little sacrifice in structure performance, yet dramatically reduced resin filling time as compared to the structurally optimized design.

2. Keywords: Topology Optimization, Manufacturing Constraint, Composite Structure, Resin Transfer Molding (RTM), Resin Filling Time

3. Introduction
The gap between the output of computer-based structure topology optimization and the final component ready for manufacturing is still considered as a barrier for further adoption of topology optimization in industries. Practically, some modifications are applied to the component generated by topology optimization to improve its manufacturability, which usually requires empirical expert knowledge. Such practice, however, is likely to yield suboptimal solutions with respect to either structure performance (*e.g.* stiffness) or component manufacturability, due to the nonlinearity of both responses to the change of component topologies. To resolve this problem, the process simulation (*e.g.* sheet metal stamping [1], injection molding [2] and casting [3]) can be incorporated to topology optimization as a tool of evaluating component manufacturability during optimization. Since the finite element based process simulation is usually computationally expensive, surrogate models of sampled process simulations are usually used as a means for approximate evaluation of component manufacturability. Nevertheless, the lack of generalizability of the traditional surrogate models to samples not similar to the training set has severely limited their applicability in topology optimization, where component geometries can undergo dramatic changes during optimization process. To overcome this limitation, this paper presents the application of a new class of surrogate models of manufacturing processes for evaluating component manufacturability during topology optimization. The model for resin filling process in resin transfer molding of composites is built using the data-driven manufacturing constraint modeling (MCM) [4] we previously developed. The model is trained with resin filling simulations of massive sampled topologies and statistical learning regression model. Thanks to the abstract topology features inspired by underlying physics of the filling process, the resulting process model is far more generalizable than the traditional surrogate models.
Resin transfer molding (RTM) is a closed mold manufacturing process of fiber reinforced composite materials. Due to the requirement of lightweight structures in automotive and aerospace industries, it has become a promising economic solution for components made of polymer composite materials. The mass production of BMW i3 (2013) whose body structures are made of carbon fiber composite with RTM process, is an example of its recent application in automotive industry. The design of RTM component is currently a challenge due to the lack of empirical experience and design for manufacturing (DFM) guidelines which are available to the components made by traditional manufacturing processes such as sheet metal stamping. The potential manufacturability issues of RTM process could be preform deformation due to compaction [5] and draping [6], racetracking [7], void formation [8], etc. In the early exploration of composite structure topologies, the resin filling time is a critical manufacturability concern which affects the product lead time, especially for mass production automotive applications. Figure 1 shows an example of two composite structures with the identical volume, material properties

and process parameters, but a large difference in resin filling time, due to the topology difference.,

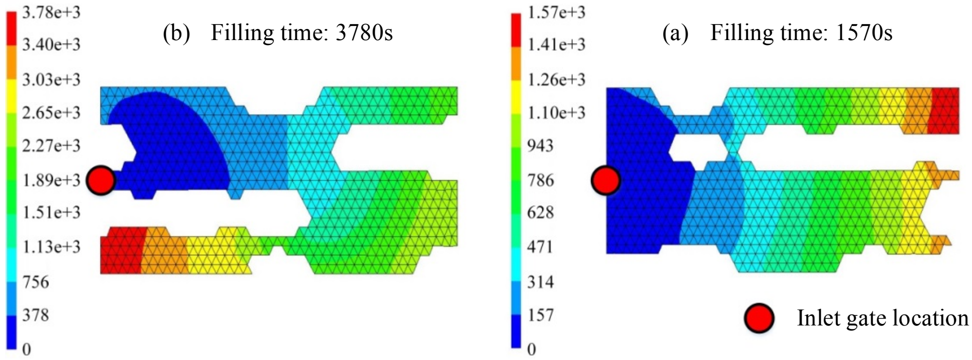

Figure 1 Examples of the non-efficient filling topology (a: 3780s) and the efficient filling topology (b: 1570s).

The rest of the paper is organized as following. Section 4 reviewed the related works on manufacturing constraint in computer-based structure optimization. Section 5 presented the data-driven predictive modeling of composite resin filling time. Section 6 discussed the result of three topology optimization case studies with the trained process model. Finally, section 7 summarized the current study and opportunities for future works.

4. Related Works

In order to improve the manufacturability of components generated by the computer-based structure optimization, many types of manufacturing constraints have been incorporated into the structure optimization loop. Several researchers proposed the algorithms to control minimum member size [9-11] and maximum length scale [12] in topology optimization. As a result, the designer gained control over member sizes which could influence the component manufacturability and cost. As for manufacturing constraints tailored for specific manufacturing processes, Harzheim *et al.* [13] developed the program TopShape to enforce casting manufacturing constraint for structure topology optimization. Zhou *et al.* [14] added the empirical sheet metal stamping manufacturing cost objective to the multi-component topology optimization. Nadir *et al.* [15] considered the manufacturing cost model of abrasive water jet process for the shape optimization. Zuo *et al.* [16] added the machining constraints to generate manufacturable topologies. Edke et al. [17] incorporated virtual machining simulation into the shape optimization of heavy load carrying components to ensure the manufacturability of the structurally optimized result.

As for the composite structure, Boccard *et al.* [18] proposed a semi-analytic model to determine the resin filling time of the preforms with isotropic permeability. In addition, Park *et al.* [19] applied the model to the composite structure optimization problem with both mechanical performance and manufacturing cost objectives. Kaufmann *et al.* [20] and Lee *et al.* [21] used the software SEER-MFG to estimate the manufacturing cost of resin transfer molding component and added it to the composite structure design process. Gantois *et al.* [22] combined the manufacturing cost with the initial multidisciplinary design optimization framework of minimum weight and maximum aerodynamic efficiency for the civil aircraft application.

However, the manufacturing process models used in these works are usually overly-simplified and tend to be conservative, in order to keep the model generalizability. We resolve it by using more accurate process simulations to evaluate structure manufacturability, and data driven predictive models to generalize the knowledge.

5. Data-Driven Composite Resin Filling Time Predictive Modeling

This section briefly summarizes the composite resin filling time predictive modeling process. The model is trained with massive process simulations and data mining of topology abstract feature representation inspired by underlying physics of the filling process. For detailed explanation, please refer to our previous work on predictive modeling of resin filling time of composite molding process [23].

5.1 Data Generation

Within the initial $2m\times1m$ bounding box (see Figure 2), 50000 random topologies are generated by Kriging level-set method [24] and labeled by their resin filling time, simulated by PAM-RTM (ESI Group). The material fraction volume, the fraction of the volume of structural materials to that of the whole bounding box is set as 0.7. The preform permeability is assumed isotropic and set as $1.0e-9\ m^2$, the thickness as $1.0e-3\ m$ and the porosity as 0.5. The inlet pressure is $1.0e5\ Pa$. As a result, the training set D_0 can be summarized as Eq.(1) below:

$$D_0 = \{\boldsymbol{x}_i, y_i |\ i = 1, 2, \dots, n\}, \tag{1}$$

where:

$\boldsymbol{x_i}$: binary bitmap representation of topology i;
$x_{ij} = 0$ if void and $x_{ij} = 1$ if filled (j: number of element in the bounding box);
$\mathrm{y_i}$: resin filling time simulation result of topology i;
n: number of training samples ($= 50000$ in this case).

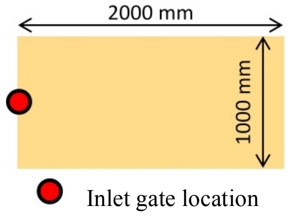

Figure 2 Bounding box for process simulation data generation.

5.2 Knowledge-Inspired Feature Representation

The performance of the predictive model depends on the quality of input features. The generalizability of the model also depends on how the topologies are represented. It is straightforward that the process model can be trained on the topology bitmap representation shown in Eq.(1). However, since the dimension of feature input is fixed as the number of elements in the initial bounding box, it is not scalable to problems with different number of element. In addition, the number of element is usually large which also poses challenges to the predictive model training process.

To resolve the scalability issue, the topology local feature representation is proposed. Figure 3 shows an example of topology local feature representation. The bounding box is divided into pieces of squared patches, each of which is matched with a member of the pre-defined feature basis by calculating the minimum Euclidean distance. As a result, the topology is represented as a vector of 18 elements. To transform the bitmap representation to local feature representation, the dimension of the input attribute reduces dramatically and no longer sensitive to the element size. However, the topology local feature representation is still not generalizable to test samples with different initial bounding box (therefore different number of patches) and different inlet gate location.

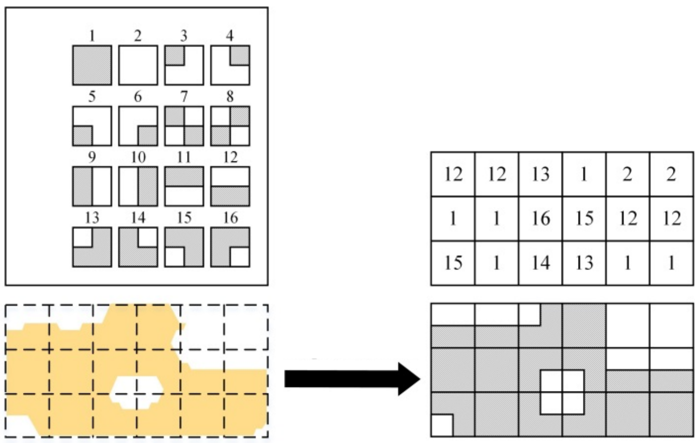

To further resolve the generalizability issue, the knowledge-inspired feature representation is proposed, which is inspired by the underlying physics of filling. An example of topology knowledge-inspired feature representation is shown in Figure 4, which consists of three major steps described below:

1) The flow through porous medium is governed by the Darcy's law which states that the flow rate per unit area is proportional to the pressure gradient. The relatively small preform area, especially at the beginning of the flow, leads to dramatically reduction of resin pressure. Therefore, to capture this phenomenon, the material fraction volume ($\boldsymbol{M}$) in each segment along the major flow route is calculated (upper right of Figure 4);
2) The length of the overall flow route also has great influence on the composite resin filling time. To capture that information, the skeleton of the initial topology is extracted using image processing thinning algorithm [25]. Then run the flood filling [26] simulation over the topology skeleton, starting at the point closest to the inlet gate location, and calculate the step count to finish the filling, defined as N (lower left of Figure 4);
3) The initial topology bitmap is then transformed to the local feature representation. Based on a pre-defined critical patch pool, the search of critical patch with different sliding window size results in a sparse vector $\boldsymbol{C}$, explained in Eq.(2) below:

$$C = [c_1, c_2, \dots, c_q], \tag{2}$$

where:

$c_i = 0$, if critical patch i not in topology;

$c_i = 1$, otherwise;

q: number of selected critical patches.

The critical patch pool is selected according to the filter-based feature selection criterion, Fisher score [27], inspired by the physics of flow that the resin filling time is effected by undesired local geometric patterns (lower right of Figure 4).

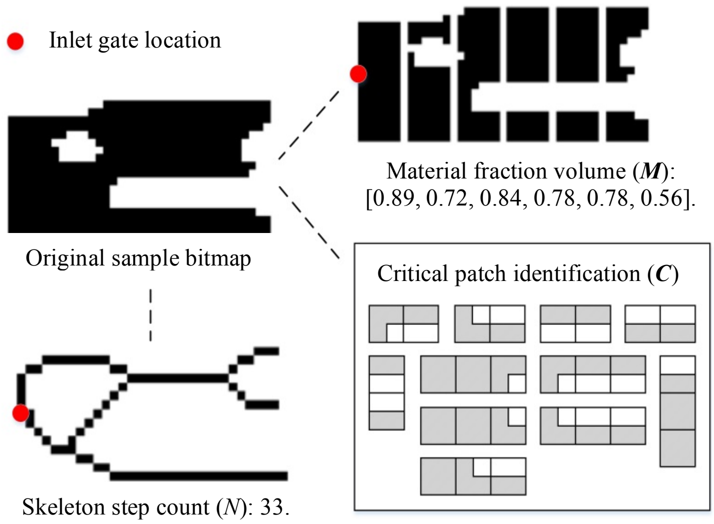

Figure 4 An example of knowledge-inspired topology feature representation.

The proposed knowledge-inspired feature representation is a more general topology representation for mold flow applications. Different from the bitmap and local feature representation, it is not sensitive to the number of element or the number of patch segment in the bounding box. In addition, it provides valuable information when the inlet gate location changes. Therefore, the trained predictive model is expected to be more generalizable to topologies not similar to the training set. Three topology optimization cases will be discussed in section 6 to test the process model robustness.

5.3 Random Forest Regression Model

After data generation and topology knowledge-inspired feature representation, the resulting transformed training set $D^{(t)}$ is summarized as Eq. (3) below:

$$D^{(t)} = \left\{\boldsymbol{x}_i^{(t)}, y_i \mid i = 1, 2, \dots, n\right\}, \tag{3}$$

where:

$\boldsymbol{x}_i^{(t)}$: knowledge-inspired feature representation of topology i, $\boldsymbol{x}_i^{(t)} = [\boldsymbol{M}, \boldsymbol{C}, N]$;

$\mathrm{y_i}$: resin filling time simulation result of topology i;

n: number of training samples ($= 50000$ in this case).

Since the input feature set is a mixture of continuous and discrete variables, the Random Forest [28] regression model is applied to the training set $D^{(t)}$ to build the resin filling time predictive model. The current model uses 50 trees with the minimum leaf size of 20 as the tuning parameters. In our previous study [23], the trained regression model was tested to be generalizable to testing samples with different inlet gate locations and initial bounding box, while the other two surrogate models trained on bitmap and local feature representations failed.

6. Topology Optimization considering Composite Resin Filling Time

The resulting manufacturing process model from section 5 is applied to the compliance minimization topology optimization problem. The multi-objective optimization problem is formulated as minimizing both structure compliance and resin filling time, summarized in Eq. (4) below:

$$\begin{gathered} \min\!: f_1(\boldsymbol{x}), f_2(\boldsymbol{x}) \\ \mathrm{s.t.}\, V(\boldsymbol{x}) = V_0, \end{gathered} \tag{4}$$

where:

$f_1(\boldsymbol{x})$: structure compliance, obtained by finite element calculation;

$f_2(\boldsymbol{x})$: resin filling time, predicted by the trained manufacturing process model from section 5;
$V(\boldsymbol{x})$: material fraction volume, set as $V_0 = 0.7$.

Since there is no known analytical sensitivity information for the random forest decision tree model, multi-objective genetic algorithm (MOGA) and Kriging level-set (KLS) [24] are used to alleviate the need for objective gradients and dramatically reduce the number of design variables. The dimension of the design variable vector $\boldsymbol{x}$ depends on the number of knot points which is independent from the mesh size. The Pareto frontier results of three test cases are generated (GA settings: 500 generations, 1000 populations per generation). The plotted objective values are normalized by the minimum value of each objective respectively. The selected non-dominated Pareto results' resin filling time responses are validated by process simulations to demonstrate the accuracy and robustness of the trained manufacturing process model.

6.1 Test Case 1: Short Cantilever

Test 1 has the identical bounding box and inlet gate location setting as the manufacturing process model training data generation, known as the *in-the-bag* test. Figure 5 below shows the support and load conditions of the short cantilever problem and its Pareto frontier result. The normalized compliance and resin filling time objective values for five selected non-dominated Pareto frontier points (green dots in Figure 5) are summarized in Table 1. The result shows a clear trade-off between the structure compliance and resin filling efficiency.

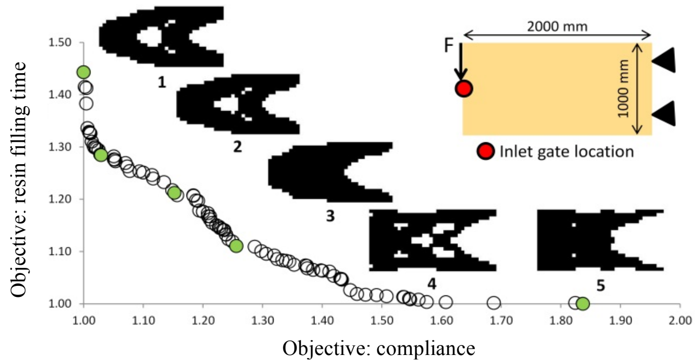

Figure 5 Pareto frontier result for test case 1.

Table 1 Objective values of selected Pareto frontier points in test case 1.

Topology	Compliance	Filling Time
1	1.00	1.44
2	1.03	1.28
3	1.15	1.21
4	1.26	1.11
5	1.84	1.00

While traditional surrogate models would produce high quality approximations for such in-the-bag tests, the proposed data-driven model also performs excellently. To validate the manufacturing process model output, the five selected topologies' resin filling time simulation results are shown in Figure 6. The simulation validation results are consistent with the predictive model outputs. As a result, if topology 2 is selected as the optimized result with both compliance and resin filling time as objectives, compared with the structurally optimized result (topology 1), it reduces the resin filling time of 4.8% (1499.75s to 1427.79s) and sacrifices the structure compliance of 2.9% (49.66 to 48.25).

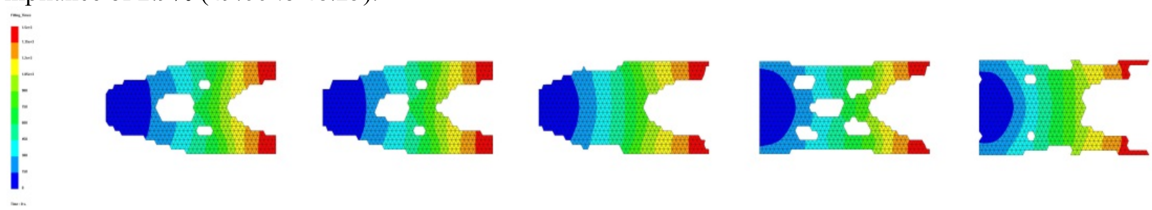

6.2 Test Case 2: Bridge

The same resin filling time manufacturing process model is also applied to another topology optimization problem with different inlet gate location as the process model training set, known as the *out-of-bag* test. It is a "bridge" problem with two-point support and mid-span load. The inlet gate location is set in the center of the structure. The resulting Pareto frontier is shown in Figure 7. The objective values for selected non-dominated points (green dots in Figure 7) are summarized in Table 2.

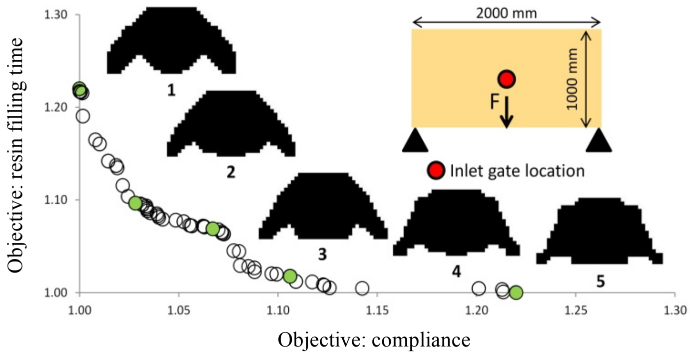

Figure 7 Pareto frontier result for test case 2.

Table 2 Objective values of selected Pareto frontier points in test case 2.

Topology	Compliance	Filling Time
1	1.00	1.22
2	1.03	1.10
3	1.07	1.07
4	1.11	1.02
5	1.22	1.00

The filling simulation result of selected Pareto points is shown in Figure 8. Though the predictive performance of out-of-bag topologies in case 2 is not as accurate as that of in-the-bag topologies in case 1, the simulation result is still consistent in terms of ranking as the process model output. It should be noted that traditional surrogate models would fail to provide reasonable approximations in this case since the gate location is different from that of the training set. As a result, if topology 2 is selected as the multi-objective optimized structure, compared with the structurally optimized result (topology 1), it reduces the resin filling time of 6.7% (410.53s to 382.85s) and sacrifices the structure compliance of 2.9% (6.93 to 7.13).

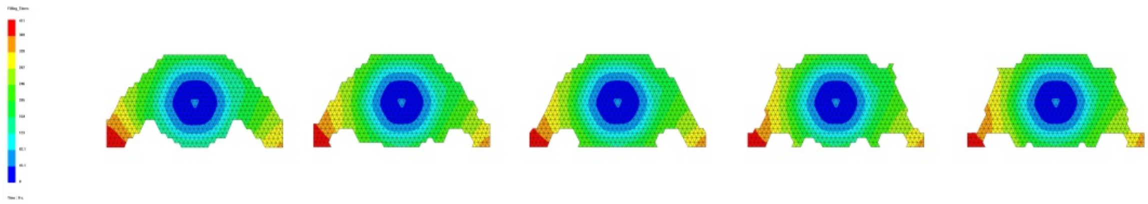

6.3 Test Case 3: Long Cantilever

Similarly, another out-of-bag test with different initial bounding box is conducted to further demonstrate the process model robustness. As discussed in section 5, while the traditional surrogate models cannot be applied due the change of input feature dimension, the proposed process model trained by more general features is still valid. The Pareto frontier result for test case 3 is presented in Figure 9. The objective values for selected non-dominated points (green dots in Figure 9) are summarized in Table 3.

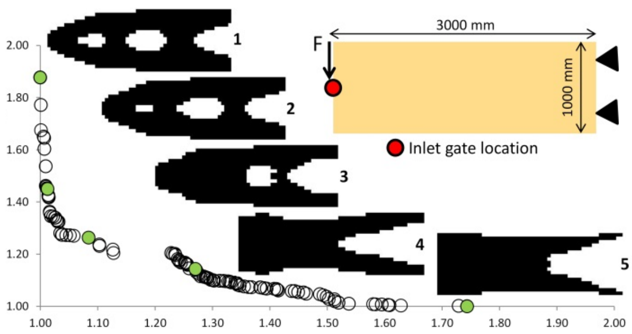

Table 3 Objective values of selected Pareto frontier points in test case 3.

Topology	Compliance	Filling Time
1	1.00	1.88
2	1.01	1.45
3	1.08	1.26
4	1.27	1.14
5	1.74	1.00

The filling simulation result of selected Pareto points for test case 3 is shown in Figure 10. The simulation result is consistent in terms of ranking as the process model output. As a result, compared with the structurally optimized topology (topology 1), if topology 2 is selected as the multi-objective optimized result, it reduces the resin filling time of 6.0% (3466.09s to 3258.48s) and sacrifices the structure compliance of 1.3% (141.29 to 143.09).

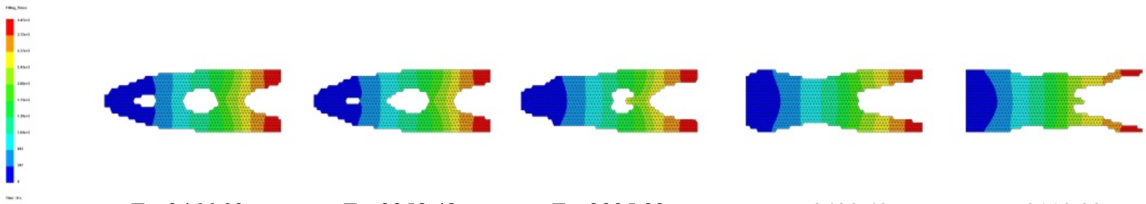

T_1=3466.09s T_2=3258.48s T_3=2935.22s T_4=2439.43s T_5=2113.39s

Figure 10 Resin transfer molding simulation validation result for selected Pareto frontier points in case 3.

According to the result of three multi-objective topology optimization test cases above, the resin filling time process model trained on features inspired by underlying physics of filling provides consistent topology filling efficiency approximation for both in-the-bag and out-of-bag tests. The model applicability to testing samples not similar to the training set demonstrates its better generalizability than traditional surrogate models which usually struggle in out-of-bag tests.

7. Discussion

This paper applies the resin filling time manufacturing process model to the compliance minimization topology optimization problem to identify topologies with improved manufacturability, yet minimum structure performance sacrifice, compared with the structurally optimized result. The scalability and generalizability of the data-driven process model is validated by three topology optimization test cases. The model applicability to samples not similar to the training set resolves the key limitation of traditional surrogate models. As of the future works, other topology representations can be studied to further improve the model predictive accuracy and generalizability. Several current assumptions should be relaxed including fixed material fraction volume and isotropic permeability of the preform. In addition, the data-driven manufacturing constraint modeling (MCM) can also be applied to other manufacturing processes (see, for example, sheet metal stamping application in reference [4]) to improve the manufacturability of components generated by computer-based structure optimization.

8. Acknowledgements

This work was supported by the U.S. Department of Energy (DOE) under Award Number DE-PI0000012, through the Clean Energy Research Center - Clean Vehicle Consortium.

9. References

[1] Tekkaya, A. E., 2000, "State-of-the-Art of Simulation of Sheet Metal Forming," Journal of Materials Processing Technology, **103**(1), pp. 14-22.

[2] Chang, R. Y., and Yang, W. H., 2001, "Numerical Simulation of Mold Filling in Injection Molding Using a Three-Dimensional Finite Volume Approach," International Journal for Numerical Methods in Fluids, **37**(2), pp. 125-148.

[3] Vijayaram, T. R., Sulaiman, S., Hamouda, A. M. S., and Ahmad, M. H. M., 2006, "Numerical Simulation of Casting Solidification in Permanent Metallic Molds," Journal of Materials Processing Technology, **178**(1-3), pp. 29-33.

[4] Zhou, Y., and Saitou, K., 2014, "Identification of Manufacturability Constraints through Process Simulation and Data Mining," ASME 2014 International Design Engineering Technical Conferences and Computers and Information in Engineering Conference.

[5] Chen, B. X., Lang, E. J., and Chou, T. W., 2001, "Experimental and Theoretical Studies of Fabric Compaction Behavior in Resin Transfer Molding," Materials Science and Engineering a-Structural Materials Properties Microstructure and Processing, **317**(1-2), pp. 188-196.

[6] Bickerton, S., Simacek, P., Guglielmi, S. E., and Advani, S. G., 1997, "Investigation of Draping and Its Effects on the Mold Filling Process During Manufacturing of a Compound Curved Composite Part," Composites Part a-Applied Science and Manufacturing, **28**(9-10), pp. 801-816.

[7] Bickerton, S., and Advani, S. G., 1999, "Characterization and Modeling of Race-Tracking in Liquid Composite Molding Processes," Composites Science and Technology, **59**(15), pp. 2215-2229.

[8] Kang, M. K., Lee, W. I., and Hahn, H. T., 2000, "Formation of Microvoids During Resin-Transfer Molding Process," Composites Science and Technology, **60**(12-13), pp. 2427-2434.

[9] Zhou, M., Shyy, Y. K., and Thomas, H. L., 2001, "Checkerboard and Minimum Member Size Control in Topology Optimization," Structural and Multidisciplinary Optimization, **21**(2), pp. 152-158.

[10] Poulsen, T. A., 2003, "A New Scheme for Imposing a Minimum Length Scale in Topology Optimization," International Journal for Numerical Methods in Engineering, **57**(6), pp. 741-760.

[11] Guest, J. K., Prevost, J. H., and Belytschko, T., 2004, "Achieving Minimum Length Scale in Topology Optimization Using Nodal Design Variables and Projection Functions," International Journal for Numerical

Methods in Engineering, **61**(2), pp. 238-254.
[12] Guest, J., 2009, "Imposing Maximum Length Scale in Topology Optimization," Structural and Multidisciplinary Optimization, **37**(5), pp. 463-473.
[13] Harzheim, L., and Graf, G., 2006, "A Review of Optimization of Cast Parts Using Topology Optimization - Ii - Topology Optimization with Manufacturing Constraints," Structural and Multidisciplinary Optimization, **31**(5), pp. 388-399.
[14] Zhou, Z. B., Hamza, K., and Saitou, K., 2014, "Decomposition Templates and Joint Morphing Operators for Genetic Algorithm Optimization of Multicomponent Structural Topology," Journal of Mechanical Design, **136**(2).
[15] Nadir, W., Kim, I. Y., and De Weck, O. L., 2004, "Structural Shape Optimization Considering Both Performance and Manufacturing Cost," 10th AIAA/ISSMO Multidisciplinary Analysis and Optimization Conference, Albany, NY, **30**.
[16] Zuo, K. T., Chen, L. P., Zhang, Y. Q., and Yang, J. Z., 2006, "Manufacturing- and Machining-Based Topology Optimization," International Journal of Advanced Manufacturing Technology, **27**(5-6), pp. 531-536.
[17] Edke, M. S., and Chang, K. H., 2006, "Shape Optimization of Heavy Load Carrying Components for Structural Performance and Manufacturing Cost," Structural and Multidisciplinary Optimization, **31**(5), pp. 344-354.
[18] Boccard, A., Lee, W. I., and Springer, G. S., 1995, "Model for Determining the Vent Locations and the Fill Time of Resin Transfer Molds," Journal of Composite Materials, **29**(3), pp. 306-333.
[19] Park, C. H., Lee, W. I., Han, W. S., and Vautrin, A., 2004, "Simultaneous Optimization of Composite Structures Considering Mechanical Performance and Manufacturing Cost," Composite Structures, **65**(1), pp. 117-127.
[20] Kaufmann, M., Zenkert, D., and Wennhage, P., 2010, "Integrated Cost/Weight Optimization of Aircraft Structures," Structural and Multidisciplinary Optimization, **41**(2), pp. 325-334.
[21] Lee, M., Ceisel, J., Liu, Z., and Mavris, D., 2012, "A Parametric, Preliminary Structural Analysis and Optimization Approach with Manufacturing Cost Considerations," 53rd Structures, Structural Dynamics, and Materials and Co-located Conferences, Honolulu, HI.
[22] Gantois, K., and Morris, A. J., 2004, "The Multi-Disciplinary Design of a Large-Scale Civil Aircraft Wing Taking Account of Manufacturing Costs," Structural and Multidisciplinary Optimization, **28**(1), pp. 31-46.
[23] Zhou, Y., and Saitou, K., 2015, "Data-Driven Predictive Model of Resin Filling Time of Composite Molding Process," ASME 2015 International Design Engineering Technical Conferences and Computers and Information in Engineering Conference, Boston, MA.
[24] Hamza, K., Aly, M., and Hegazi, H., 2014, "A Kriging-Interpolated Level-Set Approach for Structural Topology Optimization," Journal of Mechanical Design, **136**(1).
[25] Lam, L., Lee, S. W., and Suen, C. Y., 1992, "Thinning Methodologies - a Comprehensive Survey," Ieee Transactions on Pattern Analysis and Machine Intelligence, **14**(9), pp. 869-885.
[26] Soille, P., 1999, *Morphological Image Analysis : Principles and Applications*, Springer, Berlin ; New York.
[27] Duda, R. O., Hart, P. E., and Stork, D. G., 2001, *Pattern Classification*, Wiley, New York.
[28] Breiman, L., 2001, "Random Forests," Machine Learning, **45**(1), pp. 5-32.